INSTITUTO SUPERIOR TÉCNICO
Universidade Técnica de Lisboa

Structural Loads Handbook

Pedro Albuquerque
Undergraduate Student of Aerospace Engineering
Instituto Superior Técnico – Technical University of Lisbon

In collaboration with:
OGMA, Indústria Aeronáutica de Portugal, SA
Alverca do Ribatejo

October 2011

Abstract

From the design viewpoint, the determination of the loads acting on an aircraft is of outmost relevance, because their critical combinations are the designer's limit constraints.

The present work aims to enhance the work developed by the *OGMA, Indústria Aeronáutica de Portugal, SA* Engineering, Design and Modifications Office by developing a Structural Loads Handbook to enable the estimation of the maximum loads acting on an aeroplane using a thorough analysis that can work both as an alternative and a validation of the most commonly used methods, namely Computational Fluid Dynamics and Finite Element Methods commercial softwares.

So as to materialize this purpose, a number of *Microsoft Excel®* workbooks that evaluate the structural loads acting on a generic aircraft have been developed. The user is required to introduce the geometry and operational conditions of the aeroplane. The most relevant loads acting on the landing gears, wing, horizontal stabilizer, vertical stabilizer and fuselage are then analysed.

In order to demonstrate the results obtained with the methods implemented in *Microsoft Excel®* throughout this work, the shear force, bending moment and torsion are plotted along each of the main components of a *Lockheed Hercules C-130H*.

Symbols

Symbol	Description	Unit	Symbol	Description	Unit
ξ	Damping ratio	-	ω_i	Angular velocity	$\mathrm{rad/s}$
ρ	Air density	$\mathrm{kg/m^3}$	ω_n	Undamped natural frequency	$\mathrm{rad/s}$
σ_{UTS}	Ultimate tensile strength tension	N/m^2	Ω	Angular velocity	$\mathrm{rad/s}$
a	Aeroplane lift curve slope	rad^{-1}	t	Time	s
C	Damping Coefficient	Ns/m	t/c	Fuselage relative thickness	-
$C_{L_{max}}$	Maximum lift coefficient	-	U_{ref}	Reference gust velocity	$\mathrm{m/s}$
s	Laplace Transform	-	V_C	Design Cruise Airspeed	$\mathrm{m/s}$
C_p	Pressure coefficient	-	V_D	Design Dive Airspeed	$\mathrm{m/s}$
g	Gravity acceleration	m/s^2	V_S	Design Dive Airspeed	$\mathrm{m/s}$
I_i	Moment of Inertia	$\mathrm{kg/m^2}$	w	Wing loading	N/m^2
k	Spring constant	N/m	x	Displacement	m
m	Mass	kg	$\dot{x}$	Velocity	$\mathrm{m/s}$
M	Aeroplane Mass	kg	$\ddot{x}$	Acceleration	$\mathrm{m/s^2}$
n	Load factor	-			

1. Introduction

From the design viewpoint, the determination of the acting loads on an aircraft is of outmost relevance, because their critical combinations are the designer's limit constraints.

The loading conditions are those found in-flight, in the ground and during landing and take-off. Since it is impossible to investigate all the loading conditions that each aeroplane will have to withstand during its life cycle, it is normal to select those that will be critical for each member of the structure. These conditions are usually found from investigation and experience and then included in updated version of the legislations. In Europe, the current legislation for large aeroplanes is the European Aviation Safety Agency (EASA) Certification Specifications for Large Aeroplanes (CS-25).

There are four main load sources acting on an aeroplane – aerodynamic forces, inertia, ground reactions and thrust. The goal of the current work is it to determine its critical combinations. Not until all these load sources are determined shall the criticality of a particular aeroplane modification be known. Once all the loads have been determined, the challenge is to assess which critical load combinations are likely to happen to conclude about the maximum loads that may be taking place at each point.

1.1. Objectives

The present research aims to enhance the work developed by the *OGMA, Indústria Aeronáutica de Portugal, SA* Engineering, Design and Modifications Office by developing a structural loads handbook to enable the estimation of the maximum structural loads acting on an aircraft using a thorough analysis that can work as an alternative and a validation of the most commonly used methods, namely Computational Fluid Dynamics and Finite Element Methods commercial softwares.

The main purpose of this Master Thesis is to enable a much faster analysis of the maximum loads acting at each point of the aeroplane, so that modifications can be made at any point of the aeroplane without putting at risk its integrity, thus working in compliance with both the aeroplane's flight manual and the applicable legislation.

2. Structural Loads Handbook

2.1. Flight Envelope

According to both CS-25 [1] and FAR-25, the strength requirements must be met at each combination of airspeed and load factor on and within the boundaries of the representative manoeuvring envelope. This envelope, also known as V-n diagram may also be used to determine the aeroplane's structural operating limits.

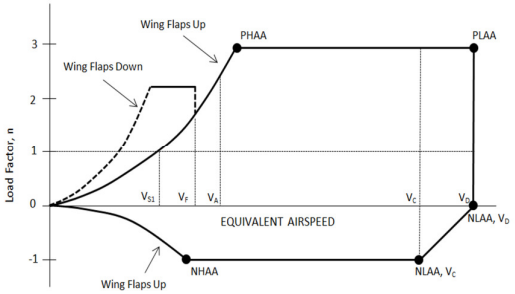

Figure 1 - Typical Flight Manoeuvring Envelope [1].

In level flight (1g) the stalling speed is given by:

$$V_{S1g} = \sqrt{\frac{Mg}{\frac{1}{2}\rho S C_{L_{max}}}} \quad (1)$$

At other load factor values, the stall speed is given by $V_S = V_{S1g}\sqrt{n}$. This will give the positive stall curve of the flight envelope. The negative design manoeuvring speed is:

$$V_{S-1g} = \sqrt{\frac{-Mg}{\frac{1}{2}\rho S C_{L_{min}}}} \quad (2)$$

At other load factor values, the stall speed is given by $V_S = V_{S-1g}\sqrt{-n}$, where n vary between zero and the minimum admissible load factor. This will give the negative stall curve.

In terms of the stresses acting on the wing on each of these conditions, it is noticeable that the PHAA will reflect the maximum compression in the upper flange of the forward longeron, which means the maximum tension will be acting on the lower

flange of the rear longeron. For the same reasons, it can be stated that the NHAA will impose the highest compression in the forward longeron lower flange and the highest tension in the rear longeron upper flange.

In the PLAA condition, the centre of pressure will be at its rear most position, which means it will be critical for compression of the rear longeron upper flange and for tension in the forward longeron lower flange. With an analogous reasoning it can be stated that the NLAA will cause maximum compression in the lower flange rear longeron and in the upper flange forward longeron.

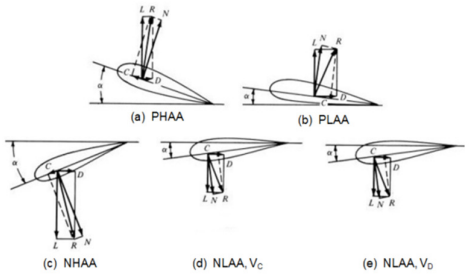

Figure 2 Limit Load Cases [2].

The gust envelope, commonly known as V-g diagram is determined in a similar pattern to the manoeuvring envelope, except that the boundaries are determined by the gust load factor at cruise airspeed (V_C) and dive airspeed (V_D). The equivalent gust velocity is defined in CS-25 [1] and FAR-25 [2] to be a function of the aeroplane's equivalent airspeed and operating altitude. The gust load factor may be computed as follows:

$$\boldsymbol{n = 1 \pm \frac{\frac{1}{2}\rho_0 V a K_g U_{ref}}{Mg/S}} \quad (3)$$

where $\boldsymbol{K_g}$ is the gust alleviation factor and is defined as:

$$\boldsymbol{K_g = \frac{0.88\frac{2w}{\rho c a g}}{5.3+\frac{2w}{\rho c a g}}} \quad (4)$$

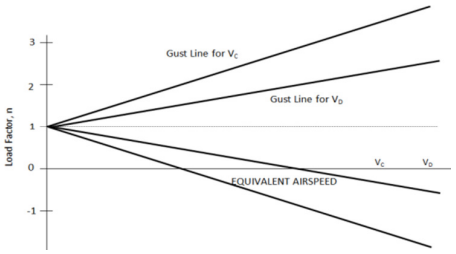

Figure 3 - Gust Envelope [1].

Once the manoeuvring and gust envelopes have been determined, the combined flight envelope should be drawn, which is shown in Figure 4. This is the most relevant plot, since it does establish the true limit loads that the aeroplane's structure may experience in the advent of being subject to gust loads coming from any direction and on any flight condition.

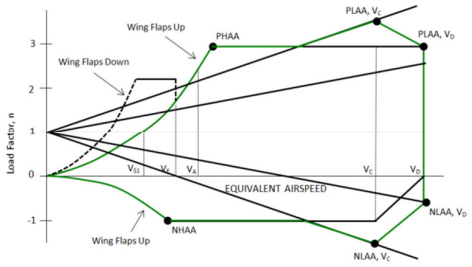

Figure 4 - Typical Combined Flight Envelope.

The limit loading conditions with a black dot in Figure 4 are critical for almost all the aircraft's structure. Each stringer and longeron is thus designed for the maximum tension or compression of each of these conditions. It is usually common place to neglect other loading conditions since the structure is likely to withstand all intermediate loadings provided that it bears the limit load conditions shown.

3. Specific Load Analysis

3.1. Landing Gear Loads

From all the loads that may act on the landing gears' structure, the most important loads involved in ground, landing and take-off must be determined.

Ground Loads

In what concerns to the landing gears ground loads, the following conditions must be investigated (in accordance with CS-25 [1]):

- Static Load
- 2-Points Braked Roll
- 3-Points Braked Roll
- Sudden braking
- Ground Turn
- Reversed Braking

- Nose wheel yaw and steering
- Unsymmetrical Braking
- Pivoting
- Towing

Landing Loads

When computing the landing gear force reactions in landing, the following conditions must be investigated [1]:

- 1-Point Landing
- 2-Points Landing
- Side Load Landing
- 3-Points Landing

According to CS-25, in order to compute the landing loads acting on the landing gears, the aeroplane lift can be assumed null. In order to determine the force acting on the landing gear the following conditions must be studied – one-point landing, two-points landing, side load landing and three-points landing.

At each landing gear a system with one or two degrees of freedom can approximate the physics of the problem. Although the system is better approximated by the system with two springs and two dampers at each landing gear, a system with a single degree of freedom per landing gear will be studied next. Nevertheless, the results derived next are extendable to the two-degrees of freedom analysis [3][4].

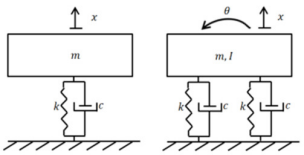

Figure 5 - Landing Gear Idealization.

The equilibrium equation is as follows:

$$\boldsymbol{m\ddot{x} + c\dot{x} + kx = 0} \quad (5)$$

The solution of the differential equation will have the form:

$$\boldsymbol{x = X_1 e^{s_1 t} + X_2 e^{s_2 t}} \quad (6)$$

Replacing this result on the equilibrium equation (5):

$$\boldsymbol{(ms^2 + cs + k)Xe^{st} = 0} \quad (7)$$

The non-trivial solution results in the roots of the polynomial between brackets on equation. Accordingly:

$$\boldsymbol{s_{1,2} = -\frac{c}{2m} \pm \frac{\sqrt{c^2 - 4mk}}{2m}} \quad (8)$$

Three different possibilities may happen, depending on the values of the aeroplane's mass, spring constant and damping coefficient.

Overdamped system response ($\xi < 1$):

$$\boldsymbol{x(t) = e^{-\xi\omega_n t}\left[x(0)\cosh\left(\omega_n\sqrt{\xi^2 - 1}t\right) + \frac{\dot{x}(0) + \xi\omega_n x(0)}{\omega_n\sqrt{\xi^2 - 1}}\sinh\left(\omega_n\sqrt{\xi^2 - 1}t\right)\right]} \quad (9)$$

Critically damped system response ($\xi = 1$):

$$\boldsymbol{x(t) = e^{-\omega_n t}[x(0)(1 + \omega_n t) + \dot{x}(0)t]} \quad (10)$$

Underdamped system response ($\xi > 1$):

$$\boldsymbol{x(t) = e^{-\xi\omega_n t}\left[x(0)\cos\left(\omega_n\sqrt{1 - \xi^2}t\right) + \frac{\dot{x}(0) + \xi\omega_n x(0)}{\omega_n\sqrt{1 - \xi^2}}\sin\left(\omega_n\sqrt{1 - \xi^2}t\right)\right]} \quad (11)$$

From the displacement response it is possible to compute the maximum loads acting on the system in each of the conditions to be analysed throughout the landing loads study.

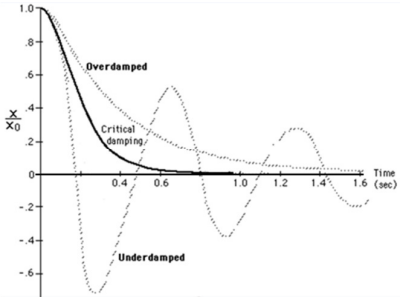

Figure 6 - Type of response.

Take-off Loads

A major concern when talking about landing gear loads arises when the landing gear is retracted. As it is known, in order to minimize noise propagation and low aerodynamic forces, most of today's aircrafts retract their landing gears immediately after take-off. Although the nose landing gears are usually retracted without changing its wheel direction, the main gears are commonly retracted inwards, which means that there will be a change in the wheel direction which can generate significant loads on the landing gear and its attaching structure. Indeed, if the wheels are still rotating at high angular speeds this can be a critical

design condition for this structure due to gyroscope effect.

If the landing gear retraction is considered a rigid body motion about an axis, the sum of moments about this point will be given by [5]:

$$\sum \boldsymbol{M_0} = \left(\dot{\boldsymbol{H}}_{\boldsymbol{0}}\right)_{xyz} + \boldsymbol{\Omega} \times \boldsymbol{H_0} \quad (12)$$

The angular momentum will be given by:

$$\begin{cases} \boldsymbol{H_x} = \boldsymbol{I_x\omega_x} - \boldsymbol{I_{xy}\omega_y} - \boldsymbol{I_{xz}\omega_z} \\ \boldsymbol{H_y} = -\boldsymbol{I_{yx}\omega_x} + \boldsymbol{I_y\omega_y} - \boldsymbol{I_{yz}\omega_z} \\ \boldsymbol{H_z} = -\boldsymbol{I_{zx}\omega_x} - \boldsymbol{I_{zy}\omega_y} + \boldsymbol{I_z\omega_z} \end{cases} \quad (13)$$

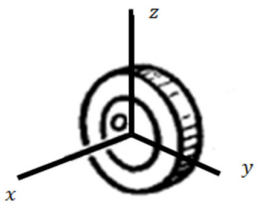

Figure 7 - Reference Axis.

Finally, and substituting the results shown on equation (13) in equation (12), and knowing that ($\Omega = \omega_y$), and recalling that the cross products of inertia will be zero due to symmetry, the expression to compute the moment will take the following form:

$$\sum \boldsymbol{M_0} = \mathbf{0} + \boldsymbol{\omega_y}\mathbf{j} \times (\mathbf{I_x}\boldsymbol{\omega_x}\mathbf{i} + \mathbf{I_y}\boldsymbol{\omega_y}\mathbf{j}) \quad (14)$$

$$\sum \boldsymbol{M_0} = -\boldsymbol{\omega_y}\mathbf{I_x}\boldsymbol{\omega_x}\boldsymbol{k} \quad (15)$$

3.2. Wing Loads

The loads on the wing are the sum of the aerodynamic lift and drag forces, as well as concentrated and distributed weight of wing-mounted engines, fuel stored and structural elements. The resulting load factor will vary within the aeroplane's flight envelope already discussed.

Symmetrical Manoeuvres

By performing an analysis of the combined flight envelope limit conditions (PHAA, PLAA, NHAA, NLAA) it is possible to address all the limit stress conditions. These results are summarized on Figure 8 and are a result of the aeroplane's centre of pressure forward shift in the case of high angles of attack and reward shift in the opposite situation.

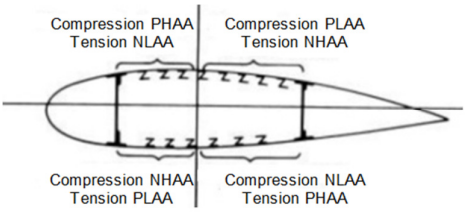

Figure 8 - Stress distribution as a function of the angle of attack.

Rolling Manoeuvre

The rolling manoeuvre analysis [7] uses the following parameters:

- Aeroplane Load Factor,(n_Z) and resulting flight wing loads;
- Maximum Roll Velocity, ($\dot{\phi}$);
- Maximum Roll Acceleration, ($\ddot{\phi}$);

The wing spanwise load distribution [7] may be considered the sum of the following increments:

- Symmetrical Loads Increments;
- Spanwise Load Distributions During Rolling Manoeuvres;
- Rolling Manoeuvre Load Factors.

Yawing Manoeuvre

The lateral manoeuvre and lateral gust requirements involve design conditions that are critical for the empennage and for the fuselage. In general, the wing structure is not critical for these kind of conditions, except for the attachment of wing/nacelles located outboard of the wing or other external stores located on the wing like bombs or missiles. According to LOMAX (1996) [7], the aerodynamic moments on an aeroplane about its rolling axis will depend on the following variables:

- Sideslip angle;
- Rolling angular velocity;
- Sideslip angular velocity;
- Spoilers' deflection;
- Ailerons' deflection;
- Rudder deflection.

3.3. Horizontal Tail Loads

The horizontal tail loads are highly dependent on the tail configuration. The three possibilities listed below apply for both the conventional and T-tail configurations:

- Integral Stabilizer with Elevator (e.g. *Airbus A320*) – In this configuration the stabilizer deflects as a whole to ensure that as the centre of gravity shifts forward or reward throughout the flight the aeroplane remains balanced with the elevator in its neutral position. This adjustment is usually done by the automatic pilot. The elevator works whenever the pilot wants to perform a pitch-up of pitch-down manoeuvre.
- Integral Stabilizer without Elevator (e.g. *F-16*) – In this configuration the whole stabilizer works to balance force moments and to manoeuvre the aeroplane with respect to its pitch axis. In spite of this Structural Loads Handbook focus on Large Aeroplanes (CS 25) and this particular stabilizer configuration is not common among these aircrafts, it will be analysed since it is the simplest configuration.
- Non-Integral Stabilizer with Elevator and Tabs (e.g. *Lockheed C-130*) – In this configuration the stabilizer as a whole does not move. Instead, the tab deflection ensures the balance of forces and moments about the CG. Once again, the elevator deflection is used to manoeuvre about the pitch axis.

Conditions to be investigated under CS-25:

- Balanced manoeuvre analysis
- Abrupt unchecked elevator condition
- Abrupt checked elevator condition

3.4. Vertical Tail Loads

The possible limit loading conditions for the vertical tail are defined on the legislation [1] and experience [7]. Accordingly:

Table 1 - Critical conditions for the vertical tail.

Flight Condition	Scheme
Manoeuvre I	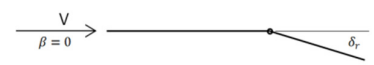
Manoeuvre II	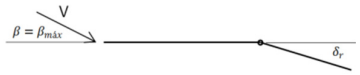
Manoeuvre III	
Engine-Out $(\boldsymbol{\delta_r = 0})$	
Engine-Out $(\boldsymbol{\beta = 0})$	

3.5. Fuselage Loads

The fuselage is a particularly critical part of the aeroplane and it is also the part in which all the loads are acting. Indeed, the fuselage loads include:

- Landing gear loads;
- Wing loads;
- Empennage loads;
- Fuselage aerodynamic loads;
- Pressurization loads;
- Inertial loads.

Landing Gears, Wing and Empennage Loads

Once all these loads have already been discussed, they only have to be transmitted to the fuselage in the attachments between these structures and the fuselage structure.

Fuselage Aerodynamics (Cross Flow)

Assuming no vorticity (cylinder twist) there will only be a drag coefficient associated with the cross flow on the cylinder. There will be a stagnation point, a point where the static pressure reaches its peak.

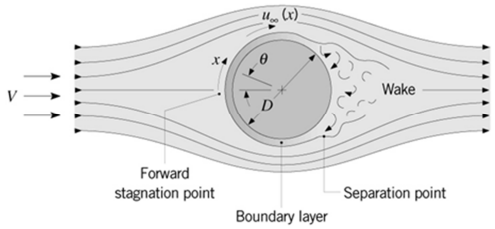

Figure 9 - Schematic representation of the cross flow acting the fuselage [6]

This point is followed by the boundary layer development under favourable pressure gradient, and hence acceleration until the free stream flow velocity. However, as the rear of the cylinder relative to the cross flow is approached, the pressure must begin to increase. Hence, there is a maximum in the pressure distribution after which the boundary layer is under the influence of an adverse pressure gradient.

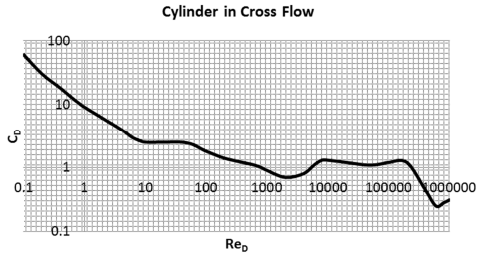

Figure 10 - Cylinder in cross flow drag coefficient as a function of the Reynolds number

Fuselage Aerodynamics (Lengthwise Flow)

For a slender body subject to axisymmetric flow it is shown [8] that on or near its surface:

$$C_p^{long} = \frac{p-p_\infty}{\frac{1}{2}\rho U_\infty^2} = -2\frac{u'}{U_\infty} - \left[\frac{S'(x)}{2\pi r}\right]^2 + O[r^4 \log(r)] \quad (16)$$

In particular, the pressure coefficient on the surface of a slender spheroid is:

$$C_p^{long} = \left(\frac{t}{c}\right)^2 \left[\frac{4x^2}{c^2-4x^2} + 2 - \log\left(\frac{4c^2}{t^2}\right)\right] \quad (17)$$

Where t is the maximum thickness, the longitudinal distance x is measured from the body centre and c is the fuselage length. It is shown [9] that there is a reasonably good agreement between the exact results and the slender-body theory approximation, especially when the body has got a high aspect ratio, as theoretically forecasted.

On the contrary of what has been done in the cross flow acting the fuselage, where it was assumed that that contribution was only meaningful in the fuselage sections 1, 2 and 4, now the fuselage must be treated as a whole, since the lengthwise flow acts it all.

NOTE: The reader should notice that although the assumptions are conservative, the three-dimensional flow structure around a cylinder in forward flow at a certain angle of attack is quite complex. This complexity makes it very hard to have good estimates for the fuselage pressure field without the use of computational fluid dynamics techniques or commercial softwares that can account for the three-dimensional flow structure around the fuselage as well as for the generation of vortexes.

Pressurization Loads

According to CS 25.365, the aeroplane structure must be strong enough to withstand the flight loads combined with pressure differentials loads from zero up to the maximum relief valve setting. This relieving valve works as a safety device that enables a decrease in the cabin pressure whenever the pressure difference between the fuselage's outer and inner skins surpasses a given admissible threshold for a particular fuselage.

Available on aeroplanes flight manuals is the Pressurization Chart that provides guidance on the difference between inner and outer skin pressure for each aeroplane operating altitude. The critical loading conditions arise when no pressure difference is felt or when the maximum admissible pressure difference is reached, which corresponds to the relief valve setting.

This maximum pressure difference can also be obtained by computing the difference between the minimum acceptable pressure for human comfort and ISA's atmosphere pressure at the aeroplane's ceiling operation.

Inertial Loads

These loads are of particular relevance in the case of a fuselage, since almost all the payload is carried on the fuselage. They will depend on the

flight condition under analysis as well as on the amount of payload being lifted. Figure 4 identifies all the limit conditions that have to be studied. These limit conditions refer to a combination of equivalent airspeed and load factor.

4. Microsoft Excel® Workbooks

Some of the methods presented so far have been adopted to build a number of interconnected *Microsoft Excel®* workbooks to expedite structural loads analysis at OGMA, *Indústria Aeronáutica de Portugal*, SA.

The set of *Microsoft Excel®* workbooks developed throughout this research [9] assess all in flight, ground, take-off and landing conditions for a generic aeroplane for each point of its main structural subsets – fuselage, wing, horizontal - stabiliser, vertical-stabiliser and landing gears. Finally, the loads are combined to obtain some of the limit loads at each point, enabling the plot of the limit shear force, bending moment and torsion loads at each point of the aeroplane.

In order to obtain these results, the user is required to input the aeroplane operational conditions as well as all its geometric data.

The instructions manuals found in appendix E of reference [9] should be carefully read.

There are three general workbooks, one in which the user can choose the system of units under use, another where the atmospheric properties are estimated from the aeroplane's maximum ceiling operation and a third one where the main aeroplane external dimensions as well as empennage arrangement are inputted.

AIR PROPERTIES - TROPOSPHERE			
INPUTS			
M (AIR) (kg/kmol)	28.8	R (J/kmol.K)	8,314.0
ALTITUDE (m)	11,000.0	R (J/kg.K)	288.3
		g (m/s2)	32.2
INPUTS		OUTPUTS	
ISA ATMOSPHERE (TROPOSPHERE h<11000m)			
Reference Values		Actual Values	
T0 (K)	288.2	T (K)	216.7
P0 (Pa)	101,325.0	P (Pa)	22,630.6
ρ0 (kg/m3)	1.225	ρ (kg/m3)	0.362
		a (m/s) Soud Speed	295.700

Figure 11 - Print screen with Microsoft Excel workbook referring to atmospheric properties

It is then possible to find a folder where the user can input data about the weight distribution on each aircraft component and a folder where the landing gear, wing, fuselage, horizontal tail and vertical tail loads are computed, according to the theoretical background already presented in order to determine the critical loads on each of these structures.

1-POINT LANDING	
INPUTS	
MLW (kg)*	59000
K - Spring Constant (N/m)*	700000
C - Damping Constant (Ns/m)*	150000
x0 (m)	-1
LEGISLATIO	
(MLW) - Limit Descent Velocity (m/s)	3.05
OUTP	
MLW	
Type of system	Underdamped
ω (Undamped) (rad/s)	3.444
Cc - Critical Damping Constant (kg/s)	406448.0287
ζ (Damping coefficient)	0.369050873
(MLW) - Fmax (N)	177856
Vz (N)*	1.78E+05
Vx (N)*	4.45E+04

Figure 12 – Print screen with the one point landing results for Maximum Landing Weight.

Finally, these loads are combined and plotted, so that the user can have a feeling on critical loads acting on the overall structure.

5. Case Study

In order to test the *Microsoft Excel®* workbooks throughout this study, the *Lockheed C-130* will be studied. An Instructions Manual has been created to facilitate the user's task when handling those workbooks [9]. The reader is encouraged to read it before looking at the results obtained to be aware of its architecture, inputs, outputs and assumptions.

Figure 13 - Portuguese Air Force C-130H

Despite being a military aircraft – which means the certification authority is the respective Air Force – the results presented next were obtained making use of EASA's CS-25. It is not uncommon that the Air Forces demand the design organizations to follow several specifications for civilian aeroplanes.

In order to make use of the Microsoft Excel® workbooks developed throughout this study, a number of inputs variables must be known [9]. Some data was obtained directly from the aeroplane flight manual, while some other data was confidential and had to be estimated.

5.1. Results

Landing Loads

Table 2 - Maximum landing loads on each landing gear.

Landing Gear	Variable	Maximum Value [N]
Nose Gear	V_z	3.28×10^5
	V_x	1.24×10^5
	V_y	1.99×10^5
Main Gear (Right)	V_z	1.70×10^6
	V_x	5.74×10^5
	V_y	5.23×10^5
Main Gear (Left)	V_z	1.70×10^6
	V_x	5.74×10^5
	V_y	5.23×10^5

Ground Loads

Table 3 – Maximum ground loads on each landing gear.

Landing Gear	Variable	Maximum Value [N]
Nose Gear	V	3.85×10^5
	D	0
	S	2.17×10^5
Main Gear (Right)	V	4.26×10^5
	D	2.79×10^5
	S	6.81×10^4
Main Gear (Left)	V	4.26×10^5
	D	2.79×10^5
	S	6.81×10^4

Wing Loads

Given the similarity between the plots of the lifting surfaces, only the shear, bending moment and torsion diagrams of the wing are presented next. Diagrams of the empennage can be found on reference [9].

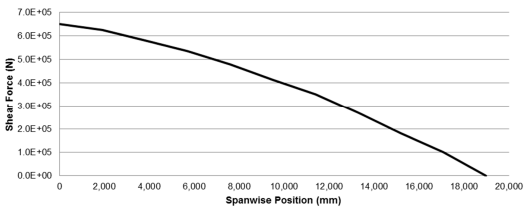

Figure 14 - Wing maximum shear force on the vertical plane – ($\boldsymbol{n_z = n_{z_{max}}}$) – (half-spanwise distribution)

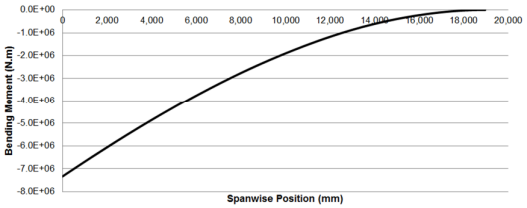

Figure 15 - Wing maximum bending moment on the vertical plane – ($\boldsymbol{n_z = n_{z_{max}}}$)

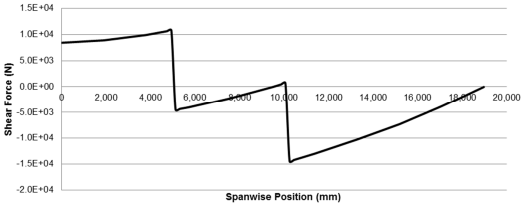

Figure 16 - Wing maximum shear force on the horizontal plane (half-spanwise distribution)

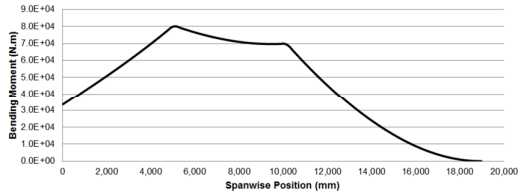

Figure 17 - Wing maximum shear force on the horizontal plane (half-spanwise distribution)

Fuselage Loads

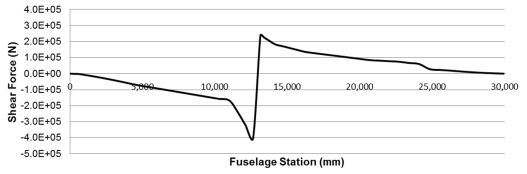

Figure 18 - Fuselage shear force in level flight (lengthwise distribution)

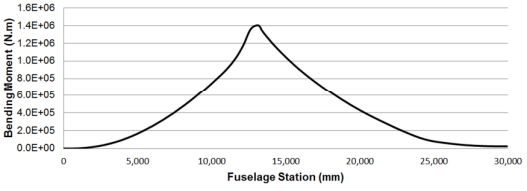

Figure 19 - Fuselage bending moment in level flight (lengthwise distribution)

6. Validation

Although the purpose of this master thesis was to work with loads without working with stresses, it must be noticed that the best way to validate the results presented so far is to determine the maximum tensile stresses working on the C-130

structure to evaluate if these values are in the order of magnitude of the tensile stress of its materials.

Some simple equations – with conservative assumptions – relating the bending moment and the maximum tensile stress were used. The results were found to be within the expected range of the order of magnitude of the 2024 and 7075 aluminium alloys – the ones used in the C-130 structure – tensile stresses and below these values, as required ($\sigma_{UTS} \approx 215MPa$ for the 2024 and $\sigma_{UTS} \approx 400MPa$ for the 7075).

7. Conclusions

Structural loads analysis is an everyday procedure for design companies all over the world. Not only the aircrafts' manufacturer companies, but also companies operating design modifications on aeroplanes. In order to enhance the methods to perform structural load analysis analytical methods capable of providing trustworthy estimates have been presented.

The generic set *Microsoft Excel®* workbooks developed throughout a six month curricular internship at *OGMA, Indústria Aeronáutica de Portugal, SA* enables determining the static loads acting on most of the aircraft to which the company´s Engineering, Design and Modifications Department works with, namely the Lockheed Hercules C-130, Lockheed Hercules P3, Embraer 134/145 and all Airbus A320 family. So as to ease the handler's use of the *Microsoft Excel®* workbooks developed, an Instructions Manual is attached to this work's report [9]. Reading this manual as well as the current report is a request for anyone wanting to work with these workbooks.

The results presented were found to be both qualitatively correct from the graphics observation and quantitatively trustworthy.

Acknowledgements

This master thesis was a collaborative work between *Instituto Superior Técnico* and OGMA, *Indústria Aeronáutrica de Portugal, SA*. I would like to thank my advisors, Professors Filipe Cunha, Luís Reis and Engineer Carlos Rodrigues for their tireless help and guidance. I am also very grateful to Professor Luís Eça, Professor Relógio Ribeiro, my friends and colleagues Bruno Tojo, Diogo Vicente and Stefano Carli and my sister Ana Albuquerque.

References

[1] **Certification Specifications for Large Aeroplanes (CS-25)**, European Aviation Safety Agency, 2009.

[2] MEGSON, **Aircraft Structures for Engineering Students**, Fourth Edition, ELSEVIER, 2006.

[3] MAIA, Nuno; MONTALVÃO, Júlio; **Vibrações e Ruído**, Instituto Superior Técnico – Universidade Técnica de Lisboa, 2011.

[4] BEARDS, C.E.; **Structural Vibration: Analysis and Damping**, ARNOLD, 1996.

[5] BEER, Ferdinand; JOHNSTION, Russel; EISENBERG, Elliot; **Vector Mechanics for Engineers – Dynamics**, 2004.

[6] DEWITT, Incropera; LAVINE, Bergman; **Fundamentals of Heat and Mass Transfer**, Sixth Edition, WILEY, 2006.

[7] LOMAX, Ted L.; **Structural Load Analysis for Commercial Transport Aircraft: Theory and Practice**, AIAA, 1996.

[8] THWAITES, Bryan; **Incompressible Aerodynamics – An Account of the Theory and Observation of the Steady Flow of Incompressible Fluid Past Aerofoils**, Wings and Other Bodies, DOVER PUBLICATIONS, INC, 1960.

[9] ALBUQUERQUE, Pedro; **Structural Loads Handbook**, Instituto Superior Técnico – Universidade Técnica de Lisboa; OGMA, Indústria Aeronáutica de Portugal, SA, 2011.